

Damped Bernstein modes in a weakly relativistic pair plasma

E. W. Laing and D. A. Diver*

Department of Physics and Astronomy, Kelvin Building, University of Glasgow, Glasgow G12 8QQ, Scotland, United Kingdom

(Received 21 April 2005; published 20 September 2005)

Relativistic Bernstein modes are not totally undamped, but have a small, negative definite imaginary frequency component that peaks where the frequency is closest to the rest cyclotron harmonic.

DOI: 10.1103/PhysRevE.72.036409

PACS number(s): 52.25.Dg, 52.25.Xz, 52.27.Ep, 52.27.Ny

I. INTRODUCTION

In our previous paper on Bernstein modes in a weakly relativistic treatment based on Maxwellian distributions [1] we claimed that contributions due to the singularities that occurred at the resonances $\gamma^2 = n^2/\hat{\omega}^2$ exactly canceled, leaving the modes undamped. However, it has since been pointed out [2] that the path of integration proposed in [1] to avoid the singularities was incorrect. The correct path should have been below the singularity on the negative \hat{p}_{\parallel} axis, and above it on the positive \hat{p}_{\parallel} axis. As a result, the contributions add, and the modes are damped.

In this paper we calculate the damping of the relativistic Bernstein modes, assuming that the damping is weak. More precisely, given that the frequency of a Bernstein wave of normalized wave number $\kappa = (2/a)^{1/2} k_{\perp} c / \Omega_0$ is $\hat{\omega} = \omega / \Omega_0$, we now write $\hat{\omega} = \hat{\omega}_r + i\hat{\omega}_i$, and assume that $|\hat{\omega}_i/\hat{\omega}_r| \ll 1$. We will use the same notation throughout as in [1], so that $a = m_e c^2 / (k_B T)$ is the relativistic parameter, and $\Omega_0 = eB_0/m_e$ is the rest cyclotron frequency for an electron or positron.

The full dispersion relation obtained in [1] is

$$\hat{\omega}^2 - 2\hat{\omega}_p^2 = \frac{4\hat{\omega}_p^2 a^{5/2}}{\sqrt{2\pi\hat{\omega}^2 k_{\perp}^2}} \sum_{n=1}^{\infty} n^4 \int_0^{\infty} d\hat{p}_{\perp} \hat{p}_{\perp} J_n^2(\hat{k}_{\perp} \hat{p}_{\perp}) e^{-a\hat{p}_{\perp}^2/2} \times \int_{-\infty}^{\infty} d\hat{p}_{\parallel} \frac{e^{-a\hat{p}_{\parallel}^2/2}}{1 + \hat{p}_{\parallel}^2 + \hat{p}_{\perp}^2 - n^2/\hat{\omega}^2}, \quad (1)$$

where $\hat{\omega}_p = \omega_p / \Omega_0$ is the normalized plasma frequency, $\hat{p}_{\parallel} = p_{\parallel} / (m_e c)$ and $\hat{p}_{\perp} = p_{\perp} / (m_e c)$.

Consider the properties of the second integral in Eq. (1). In the limit $|\hat{\omega}_i/\hat{\omega}_r| \ll 1$,

$$\frac{n^2}{\hat{\omega}^2} \approx \frac{n^2}{\hat{\omega}_r^2} \left(1 - 2i \frac{\hat{\omega}_i}{\hat{\omega}_r} \right). \quad (2)$$

Hence the integral becomes

$$I = \int_{-\infty}^{\infty} d\hat{p}_{\parallel} \frac{e^{-a\hat{p}_{\parallel}^2/2}}{1 + \hat{p}_{\parallel}^2 + \hat{p}_{\perp}^2 - n^2/\hat{\omega}_r^2 + 2in^2\hat{\omega}_i/\hat{\omega}_r^3}. \quad (3)$$

For convenience, define

$$b_n^2 = n^2/\hat{\omega}_r^2 - 1 \quad (4)$$

so that it is apparent that a different treatment of the integral I is required, depending on the sign of b_n^2 and the relative sizes of b_n^2 and \hat{p}_{\perp}^2 .

We will use throughout the notation

$$x_n^2 = ab_n^2/2, \quad (5)$$

$$y_n = an^2\hat{\omega}_i/\hat{\omega}_r^3 < 0, \quad (6)$$

$$v^2 = a\hat{p}_{\parallel}^2/2, \quad (7)$$

$$x^2 = x_n^2 - a\hat{p}_{\perp}^2/2. \quad (8)$$

Case (i) $b_n^2 > 0$, $b_n^2 > \hat{p}_{\perp}^2$

The integral terms in Eq. (1) can be written in the simpler form

$$I = \sqrt{2/a} \int_0^{x_n} x e^{-x^2+x^2} J_n^2(\kappa\sqrt{x^2-x^2}) dx \int_{\Gamma} \frac{e^{-v^2} dv}{v^2 - x^2 + iy_n}, \quad (9)$$

in which Γ is the Landau contour given in Fig. 1. The poles are at $\pm v_0$, where $v_0 = \sqrt{x^2 - iy_n}$.

For the singular integral in Eq. (9), the contribution from the poles is given by

$$-2\pi i \frac{e^{-x^2+iy_n}}{v_0} \quad (10)$$

using the Residue theorem. The integration along the real line then yields

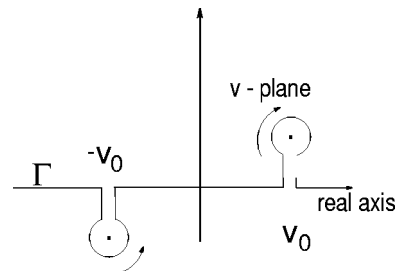


FIG. 1. Definition of the contour for the integral in Eq. (9).

*Corresponding author. Email address: d.diver@physics.gla.ac.uk

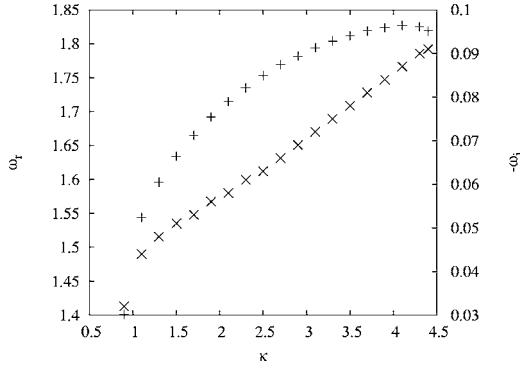


FIG. 2. Pluses (+) show the upper loop of the dispersion curve $\hat{\omega}_r$ (left y axis) vs κ (x axis) for $a=10$, and $1 < \hat{\omega}_r < 2$. The crosses (x) show how $-\hat{\omega}_i$ (right y axis) varies as a function of κ along the dispersion curve.

$$\int_{-\infty}^{\infty} \frac{(v^2 - x^2)e^{-v^2} dv}{(v^2 - x^2)^2 + y_n^2} - iy_n \int_{-\infty}^{\infty} \frac{e^{-v^2} dv}{(v^2 - x^2)^2 + y_n^2} \quad (11)$$

with all other contributions canceling. Note that the integrals above are both real.

Case (ii) $b_n^2 > 0$, $b_n^2 < \hat{p}_\perp^2$

Here the \hat{p}_\parallel integral takes the form

$$\int_{-\infty}^{\infty} \frac{e^{-v^2} dv}{v^2 + x^2 + iy_n} \quad (12)$$

and is nonsingular. This integral can be expressed in terms of real and imaginary parts as

$$\int_{-\infty}^{\infty} \frac{e^{-v^2}(v^2 + x^2)}{(v^2 + x^2)^2 + y_n^2} dv - iy_n \int_{-\infty}^{\infty} \frac{e^{-v^2}}{(v^2 + x^2)^2 + y_n^2} dv. \quad (13)$$

When $y_n=0$, the second integral vanishes, as expected.

Case (iii) $n < \hat{\omega}_r$

This is similar to case (ii), but now $b_n^2 < 0$; the \hat{p}_\perp integral is as before, subject to this proviso.

The dispersion relation for frequency $m-1 < \hat{\omega}_r < m$ where $m \geq 2$ is an integer and $C = 8\sqrt{\pi}\hat{\omega}_p^2 a / \kappa^2$ can be written

$$\hat{\omega}_r^2 + 2i\hat{\omega}_i\hat{\omega}_r - 2\hat{\omega}_p^2 = \frac{C}{\hat{\omega}_r^2} \left(1 - 2i\frac{\hat{\omega}_i}{\hat{\omega}_r} \right) \times \left[\sum_{n=1}^{m-1} n^4 A_n^{\text{III}} + \sum_{n=m}^{\infty} n^4 (A_n^{\text{I}} + A_n^{\text{II}} - iB_n) \right] \quad (14)$$

in which

$$A_n^{\text{I}} = e^{-x_n^2} \int_0^{x_n} x e^{x^2} J_n^2(\kappa\sqrt{x_n^2 - x^2}) [q_1(x, y_n) - iy_n q_2(x, y_n)] dx, \quad (15)$$

$$A_n^{\text{II}} = e^{-x_n^2} \int_0^{\infty} x e^{x^2} J_n^2(\kappa\sqrt{x_n^2 + x^2}) [p_1(x, y_n) - iy_n p_2(x, y_n)] dx, \quad (16)$$

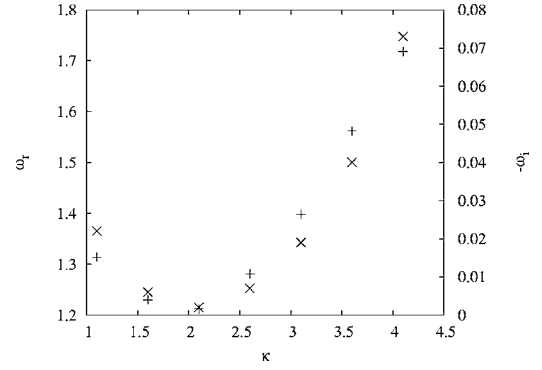


FIG. 3. Caption as for Fig. 2, showing the real and imaginary parts on the lower loop of the same dispersion curve.

$$A_n^{\text{III}} = e^{-x_n^2} \int_{|x_n|}^{\infty} x e^{-x^2} J_n^2(\kappa\sqrt{x^2 + x_n^2}) \times [p_1(x, y_n) - iy_n p_2(x, y_n)] dx, \quad (17)$$

$$B_n = 2e^{-x_n^2} \int_0^{x_n} \frac{x J_n^2(\kappa\sqrt{x_n^2 - x^2})}{\sqrt{x^2 - iy_n}} e^{iy_n} dx, \quad (18)$$

and where the following additional function definitions have been used:

$$p_1(x, y) = \frac{1}{\pi} \int_{-\infty}^{\infty} dv \frac{e^{-v^2}(v^2 + x^2)}{(v^2 + x^2)^2 + y^2}, \quad (19)$$

$$p_2(x, y) = \frac{1}{\pi} \int_{-\infty}^{\infty} dv \frac{e^{-v^2}}{(v^2 + x^2)^2 + y^2}, \quad (20)$$

$$q_1(x, y) = \frac{1}{\pi} \int_{-\infty}^{\infty} dv \frac{e^{-v^2}(v^2 - x^2)}{(v^2 - x^2)^2 + y^2}, \quad (21)$$

$$q_2(x, y) = \frac{1}{\pi} \int_{-\infty}^{\infty} dv \frac{e^{-v^2}}{(v^2 - x^2)^2 + y^2}. \quad (22)$$

Note that in the limit $y_n \rightarrow 0$, $p_1 \rightarrow e^{x^2} \text{erfc}(x)$, $q_1 \rightarrow ie^{-x^2} \text{erf}(ix)$, and A_n^{II} and A_n^{III} become purely real; these then agree with the definitions given in Eqs. (48) and (49) of [1]. The real part of A_n^{I} similarly agrees with Eq. (47) of [1], but there is an imaginary contribution from the changed contour.

The procedure now, as discussed earlier, is to extract the real and imaginary parts of the dispersion relation and to make the assumption that the real part is relatively unchanged from our earlier paper [1]. In this way, we can use the imaginary part of the dispersion relation to define an implicit relationship that will yield $\hat{\omega}_i$ as a function of $\hat{\omega}_r$ and the plasma parameters. It will turn out that we must retain the effects of y_n beyond the linear approximation in order to avoid singular integrals. This is not the case when considering the real part, hence justifying the approximation of setting $\hat{\omega}_i=0$ there.

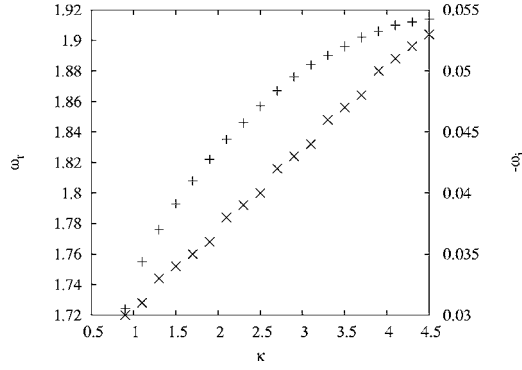


FIG. 4. Pluses (+) show the upper loop of the dispersion curve $\hat{\omega}_r$ (left y axis) vs κ (x axis) for $a=20$, and $1 < \hat{\omega}_r < 2$. The crosses (x) show how $-\hat{\omega}_i$ (right y axis) varies as a function of κ along the dispersion curve.

In order to separate the real and imaginary parts of the dispersion relation, we introduce the following notation for A_n^I :

$$A_n^I = A_{n1}^I - iy_n A_{n2}^I, \quad (23)$$

$$A_{n1}^I = e^{-x_n^2} \int_0^{x_n} x e^{x^2} J_n^2(\kappa \sqrt{x_n^2 - x^2}) q_1(x, y_n) dx, \quad (24)$$

$$A_{n2}^I = e^{-x_n^2} \int_0^{x_n} x e^{x^2} J_n^2(\kappa \sqrt{x_n^2 - x^2}) q_2(x, y_n) dx, \quad (25)$$

with the obvious extension to A_n^{II} and A_n^{III} .

For B_n , we note that

$$(x^2 - iy_n)^{-1/2} = \frac{\sqrt{r_n + x^2} - i\sqrt{r_n - x^2}}{\sqrt{2}r_n}, \quad (26)$$

$$r_n^2 = x^4 + y_n^2, \quad (27)$$

$$y_n < 0, \quad (28)$$

and so we can write

$$B_n = B_{n1} + iB_{n2}, \quad (29)$$

$$B_{n1} = \sqrt{2} e^{-x_n^2} \int_0^{x_n} dx \frac{x}{r_n} J_n^2(\kappa \sqrt{x_n^2 - x^2}) \times [\sqrt{r_n + x^2} \cos y_n + \sqrt{r_n - x^2} \sin y_n], \quad (30)$$

$$B_{n2} = \sqrt{2} e^{-x_n^2} \int_0^{x_n} dx \frac{x}{r_n} J_n^2(\kappa \sqrt{x_n^2 - x^2}) \times [\sqrt{r_n + x^2} \sin y_n - \sqrt{r_n - x^2} \cos y_n]. \quad (31)$$

With this notation we can collect the imaginary terms in the dispersion relation to get

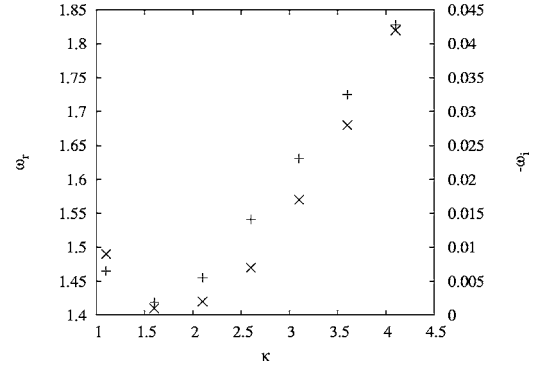


FIG. 5. Caption as for Fig. 4, showing the real and imaginary parts on the lower loop of the same dispersion curve.

$$2i\hat{\omega}_r\hat{\omega}_i = -i\frac{C}{\hat{\omega}_r^2} \left[\sum_{n=1}^{m-1} n^4 y_n A_{n2}^{III} + \sum_{n=m}^{\infty} n^4 y_n (A_{n2}^I + A_{n2}^{II}) + \sum_{n=m}^{\infty} n^4 B_{n1} \right] - i\frac{2C\hat{\omega}_i}{\hat{\omega}_r^3} \left[\sum_{n=1}^{m-1} n^4 A_{n1}^{III} + \sum_{n=m}^{\infty} n^4 (A_{n1}^I + A_{n1}^{II}) + \sum_{n=m}^{\infty} n^4 B_{n2} \right]. \quad (32)$$

Now since we have assumed that $|\hat{\omega}_i/\hat{\omega}_r| \ll 1$, and therefore that the real part of the dispersion relation can be calculated by ignoring $\hat{\omega}_i$ contributions, we have

$$\hat{\omega}_r^2 - 2\hat{\omega}_p^2 = \frac{C}{\hat{\omega}_r^2} \left[\sum_{n=1}^{m-1} n^4 A_{n1}^{III} + \sum_{n=m}^{\infty} n^4 (A_{n1}^I + A_{n1}^{II} + B_{n2}) \right]. \quad (33)$$

This allows us to simplify the expression for $\hat{\omega}_i$:

$$\hat{\omega}_i = \frac{-C \sum_{n=m}^{\infty} n^4 B_{n1}}{4\hat{\omega}_r(\hat{\omega}_r^2 - \hat{\omega}_p^2) + \frac{aC}{\hat{\omega}_r^3} \left[\sum_{n=1}^{m-1} n^6 A_{n2}^{III} + \sum_{n=m}^{\infty} n^6 (A_{n2}^I + A_{n2}^{II}) \right]}. \quad (34)$$

Note that Eq. (34) defines $\hat{\omega}_i$ implicitly, since $\hat{\omega}_i$ appears in functional dependencies on the right-hand side. To solve Eq. (34) for $\hat{\omega}_i$ requires an iterative scheme, converging on the true value. The results of such a scheme applied to the cases of $a=10$ and $a=20$, for frequencies in the range $1 < \hat{\omega}_r < 2$ and $2 < \hat{\omega}_r < 3$ and for $\hat{\omega}_p=3$, are shown in Figs. 2–7. As in [1], harmonics above the sixth order could be neglected for these cases.

It is possible to derive a very simple approximation for the right-hand side of Eq. (34). Noting that A_{m2}^I is dominant among the terms in the denominator (by virtue of its dependence on the function q_2), and similarly B_{m1} is the largest contributor to the numerator, it is possible to write

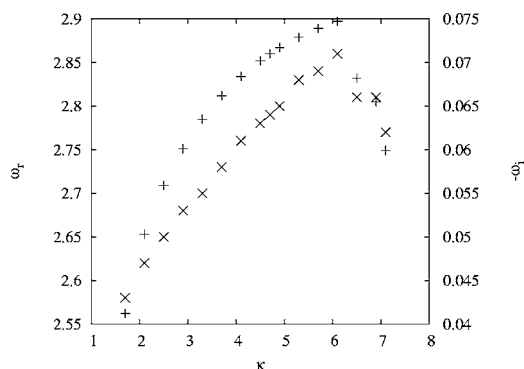


FIG. 6. Pluses (+) show the upper loop of the dispersion curve $\hat{\omega}_r$ (left y axis) vs κ (x axis) for $a=20$, and $2 < \hat{\omega}_r < 3$. The crosses (x) show how $-\hat{\omega}_i$ (right y axis) varies as a function of κ along the dispersion curve.

$$\hat{\omega}_i \approx -\frac{\hat{\omega}_r^3 B_{m1}}{am^2 A_{m2}^1} \quad (35)$$

if we retain only these dominant terms and if we neglect the term $4\hat{\omega}_r(\hat{\omega}_r^2 - \hat{\omega}_p^2)$ compared with $aCn^6 A_{m2}^1 / \hat{\omega}_r^3$. Using the definition of y_n from Eq. (6), we have eventually

$$y_m \approx -\frac{B_{m1}}{A_{m2}^1} \quad (36)$$

which generally overestimates the value of $|\hat{\omega}_i|$ by up to 20% when compared with the result of retaining all the relevant summation terms.

II. SUMMARY

This short paper updates our original calculations [1] by showing that Bernstein modes in relativistic pair plasmas are indeed damped, albeit very weakly. The classical electron-ion picture suggests that this damping should occur close to

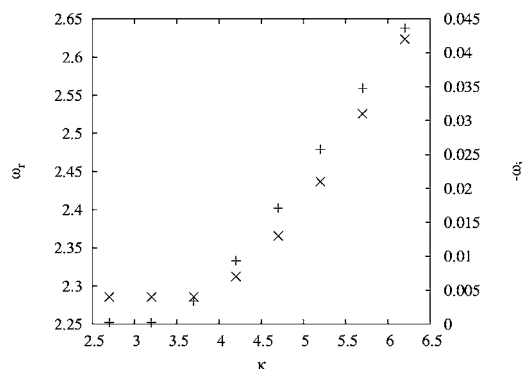


FIG. 7. Caption as for Fig. 6, showing the real and imaginary parts on the lower loop of the same dispersion curve.

the classical cyclotron resonances at $\omega \approx n\omega_c$ [3]. Our computed damping terms are largest closest to the cyclotron harmonics on the upper loop of each dispersion curve; $\hat{\omega}_i$ is comparatively smaller on the lower branch mainly because x_m is larger in that lower frequency part of the curve, and so A_{m2}^1 is more dominant than B_{m1} , leading to a smaller $\hat{\omega}_i$. This can readily be seen from the simple approximation given in Eq. (36).

Note also that we have shown in earlier work [1] that relativistic effects significantly change the shape and location of the dispersion curves for pair-plasma Bernstein modes such that they do not remain localized near a particular harmonic. In fact, most of the Bernstein mode dispersion curves are free from significant damping, and therefore the associated waves propagate largely without hindrance.

ACKNOWLEDGMENTS

It is a pleasure to acknowledge valuable and constructive comments from R. A. Cairns and C. N. Lashmore-Davies. We are grateful to PPARC for partial funding of this research.

[1] D. A. Keston, E. W. Laing, and D. A. Diver, Phys. Rev. E **67**, 036403 (2003).

[2] R. A. Cairns and C. N. Lashmore-Davies (private communication).

[3] R. A. Cairns and C. N. Lashmore-Davies, *14th Topical Conference on Radio Frequency Power in Plasmas*, edited by T. K. Mau and J. deGrassie (AIP, Melville, NY, 2001), CP595, p. 430.